Seventh International Conference on CFD in the Minerals and Process Industries
CSIRO, Melbourne, Australia
9-11 December 2009

NUMERICAL SIMULATION OF MAGNESIUM PRODUCTION BY THE PIDGEON PROCESS PART I: A NEW MODEL FOR MAGNESIUM REDUCTION PROCESS IN A HORIZONTAL RETORT

R.B. LI, J.J. WEI, L.J. GUO*, and S.J. ZHANG

State Key Laboratory of Multiphase Flow in Power Engineering, Xi'an Jiaotong University, Xi'an 710049, China
*corresponding author, E-mail address: lj-guo@mail.xjtu.edu.cn

ABSTRACT

A new model was developed to actually describe the magnesium reduction process in a horizontal retort from the perspective of chemical reaction kinetics. The shrinking non-reacted core model was kinetically modified to describe the reduction process, and the time-dependant activation energy was calculated by fitting the experimental data. The magnesium reduction heat was calculated in a piecewise manner for different temperature intervals according to the physical reduction process. A simulation for an industrial horizontal solid cylinder retort by using the new model indicated that our model is feasible. The temperature in the retort and the performance of Mg reduction process in terms of the Mg reduction rate and the heat absorption power were predicted. The prediction shows that the temperature has an increase at the first 1～2 hours, and the Mg reduction rate and the heat absorption power have a rapid increase in this period. Additionally, the influence of the heating temperature on the performance is investigated.

NOMENCLATURE

c_p	Specific heat capacity of the reactant
E	Activation energy
k	Kinetics reaction constant
k_0	Proportional coefficient
M	Maximum magnesium production per unit volume
r_0	Radius of the retort
R	Universal gas constant
S_r	Reaction source term
T	Reaction time
ρ	Effective density
λ	Effective thermal conductivity of the reactant
α	Reduction rate
α_1	Reduction rate of the reaction (10)
α_2	Reduction rate of the reaction (12)
ψ_1	Thermal energy needed per unit mass of magnesium production in stage 2) when calculating the reaction heat
ψ_2	Latent heat of magnesium vapor

INTRODUCTION

Magnesium (Mg) and its alloys will become the material of choice as designers strive to improve energy efficiency in transportation because of their favorable combination of tensile strength, elastic modulus, low density, high strength-to-weight ratios and high damping capacity. The world demand for magnesium has been increasing about 10% per year over the last ten years (Brown,2009). China, the largest producer of primary magnesium in the world, supplies 40-50% of the demand for magnesium, but it is also plagued by serious energy and environmental issues. The calculated energy efficiency of the magnesium production process is ~12%, and the global warming impact is $CO_{2\text{-eq}}$/kg of Mg ingot (Ramakrishnan and Koltun,2004). Development of a high-efficiency, economical, and low-pollution technology for magnesium production will be needed to meet the rapidly growing world demand and to reduce the emissions.

There are two major process routes for magnesium production in industry. One is to recover magnesium chloride from the raw materials and converts it to metal through molten salt electrolysis; the other is to reduce magnesium oxide at high temperature using reducing agents, such as ferrosilicon, aluminium or carbon. The Pidgeon process is a thermal reduction process, which produces magnesium from calcined dolomite under a vacuum pressure of ~10 Pa and at a temperature of 1150~1200℃ using ferrosilicon as a reducing agent. A small quantity of calcium fluoride is added as a catalyst. The whole process is carried out in a refractory brick furnace which consists of a number of cylindrical retorts. The finely ground reactant compound (mixture of calcined dolomite, ferrosilicon and fluorspar) is charged into these retorts vacuumed by the pump, and then sealed by covers and heated up. As the temperature of the reactant compound rises up, the magnesium reduction reaction occurs and the magnesium vapor generates about 4~10 hours later. The yielded magnesium vapor is transported from the reduction section to the crystalline section of the retort and then condenses in crystalline form on the water cooling jacket of the retort. Figure 1 shows schematically the structure of an industrial horizontal solid retort for magnesium production.

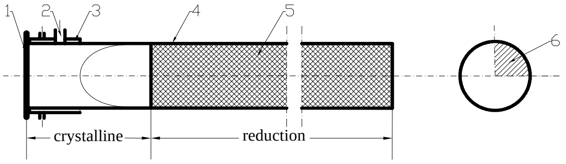

1. Cover 2. Vacuum pump 3. Cooling jacket 4. Retort 5. Reactant compound 6. Computational domain

Figure 1: Schematic structure of horizontal solid retort

There are several experimental and numerical researches on magnesium reduction in the retort. Liu and Xu (1995) analyzed in detail the heat transfer of briquette packed layer in the retort, and gave the effective thermal conductivity. Morsi et al. (2002) studied the effect of parameters, such as silicon stoichiometry, temperature, molar ratios of calcium oxide/magnesium oxide, etc, on the magnesium reduction reaction under an inert atmosphere, and obtained constant apparent activation energy for reduction. They offered useful thermophysical properties for development of the magnesium reduction models. Liang et al. (2006) studied temperature distribution in the retort only from the perspective of heat transfer without considering the Magnesium reduction reaction by simulation method. By taking the magnesium reduction reaction into account, Xie et al. (2006) assumed the magnesium reduction reaction heat to be a constant, and Yu et al. (2002) treated the reaction heat as a function of temperature, which was derived from the free energy of the magnesium reduction reaction. These simplified treatments were inadequate to simulate the magnesium reduction process accurately, so it is necessary to develop a reliable physical model for simulating the process.

In this paper, a new model for the magnesium reduction was developed from the perspective of chemical reaction kinetics, which is very distinctive compared with the existing models. The shrinking non-reacted core model was employed and kinetically modified to describe the reduction process. The time-dependant activation energy was calculated by fitting the calculated magnesium reduction rate from the model with the experimental data. Finally, the magnesium reduction reaction heat was calculated as a piecewise manner for different temperature intervals according to the physical reduction process.

PHYSICAL MODEL

Magnesium reduction reaction

Kinetically modified shrinking non-reacted core model

The calcined dolomite is finely ground and mixed in a specific ratio with finely ground ferrosilicon. A small quantity of calcium fluoride is added into the mixture as a catalyst. The mixture or compound is then briquetted and conveyed to the retort for reduction. The overall reaction is described as follows:

$$\begin{aligned} &2(\mathrm{MgO}\cdot\mathrm{CaO})_{(s)} + (\mathrm{Fe}\cdot\mathrm{Si})_{(s)} \\ &\longrightarrow 2\mathrm{Mg}_{(g)} + (2\mathrm{Ca}\cdot\mathrm{SiO}_3)_{(s)} + \mathrm{Fe}_{(s)} \end{aligned} \tag{1}$$

Experimental analysis demonstrates that the Mg reduction reaction is a gradual process advancing from exterior of the briquette to interior (Xiong, Zhou et al.,2005). At one time instant, the reduction reaction occurs only in a certain region of the briquette, and the outside of the region is fully reacted while the inside of the region is not reacted. Since the thickness of the region is far smaller than the radius of the briquette, the reaction can be considered to occur at the interface where is in a constant temperature, the shrinking non-reacted core model can be used to describe this process in the retort. The reaction model can be expressed as follows,

$$\alpha = 1 - \left(1 - \frac{kt}{3}\right)^3 \tag{2}$$

$$\frac{d\alpha}{dt} = k(1-\alpha)^{2/3} \tag{3}$$

$$k = k_0 \exp\left(-\frac{E}{RT}\right) \tag{4}$$

As we know, the component and the temperature of the briquette will vary as the reduction reaction proceeds, resulting in different activation energy E at different time. Therefore, the constant apparent activation energy given by Morsi et al.(2002) can not characterize the Mg reduction reaction process accurately. In the present study, we calculate the activation energy E by fitting the reduction rate α with the experimental data.

From Eqs. (2) and (4), we can see that the reduction rate α is a function of the reaction time t, the reaction temperature T and the activation energy E, which can also be written as

$$\alpha = \alpha(t,T,E) \tag{5}$$

Consequently, the expression of the activation energy E can be derived from Eq. (5) and expressed as

$$E = E(\alpha,t,T) = -RT\ln\frac{3\left(1-\sqrt[3]{1-\alpha}\right)}{k_0 t} \tag{6}$$

It is not difficult to determine the activation energy E if we have the measured reduction rate of Mg at different times and temperatures. Fortunately, the experimental data can be obtained from Xu and Yuan (1991), some of their data is illustrated in Figure 2.

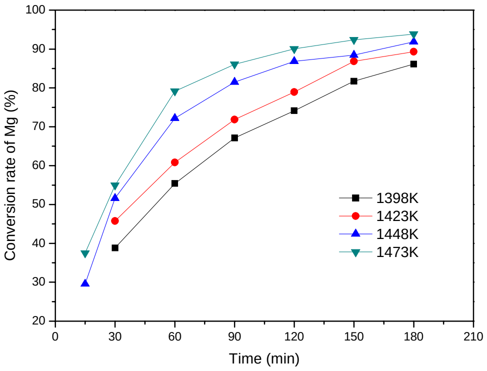

Figure 2: Experimental data of reduction rate with the time and temperature

From Eq. (5) we can see that the reduction rate α is also a function of time t and temperature T, and Eq. (6) can be further expressed as

$$E = E(t,T) \tag{7}$$

The calculated activation energy E at different times and temperatures is also illustrated with symbols in Figure 3. From the illustration, we can see that it will be a complicated equation if directly fitting the activation energy E as a function of the reaction time t and temperature T. Therefore, two simplified treatments are applied to obtain an expression for E,

1) The activation energy E at different temperatures but at the same time is linearly averaged because there is a small fluctuation of E shown in Figure 3, and thus Eq. (7) can be simplified as

$$E = E(t) \tag{8}$$

2) The activation energy is unchanged when the time is beyond the experimental time.

Based on the above treatments, the equation of the averaged activation energy *E* after fitting can be expressed as follows

$$E = \begin{cases} 66691.31 & t \le 15\,\text{min} \\ \begin{aligned} &64605.507 + 148.707t \\ &- 0.664t^2 + 0.00135t^3 \end{aligned} & 15\,\text{min} < t \le 210\,\text{min} \\ 79065.39 & t > 210\,\text{min} \end{cases} \tag{9}$$

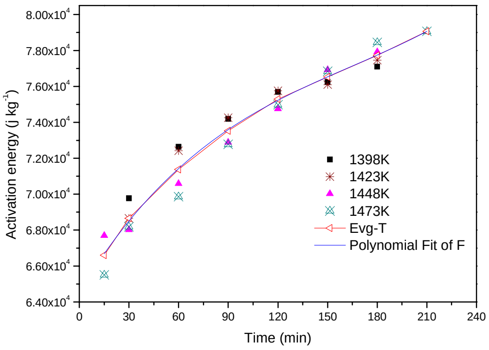

Figure 3: Correlation of the activation energy with the reaction time and temperature

Reduction reaction heat

The reaction of Eq. (1) is a solid-state endothermic reaction under vacuum and at high temperatures (Morsi, El Barawy et al.,2002). In industrial production, the vacuum pressure is maintained at about 1~10 Pa and the temperature in the range of 1100~1200℃.

Before modelling, two problems must be taken into consideration. One is the onset temperature of the Mg reduction reaction. Halmann et al. (2008) gives the calculated correlation between the onset reaction temperature and the vacuum pressure for the reduction reaction. It shows that the onset temperature is 1158 K at 10 Pa. Considering non-stoichiometric mixture, we determine the onset temperature to be 1223 K from actual industrial production. Another problem is about the boiling point of Mg. It is 1383 K at this vacuum pressure. And then, we divide the reduction process into three stages:

1) 300 K (the charging temperature)~1223 K, the compound is only heated up. It is a simple temperature rising process. The reaction heat is zero.

2) When the temperature of the compound reaches 1223 K, the Mg reduction reaction will begin, but proceed slowly. In this stage, the reaction equations can be described as:

$$\begin{aligned} &2(\mathrm{MgO \cdot CaO})_{(s)} + (\mathrm{Fe \cdot Si})_{(s)} \\ &\longrightarrow 2\mathrm{Mg}_{(l)} + (2\mathrm{Ca \cdot SiO_3})_{(s)} + \mathrm{Fe}_{(s)} \end{aligned} \tag{10}$$

This is different from the reaction of Eq. (1) in the phase of Mg. At this moment, the Mg produced is in liquid state, and does not vaporize since the temperature is lower than the boiling point of Mg. Accordingly, there is only a small reaction heat, and the temperature would still increase because of the high heat transfer rate.

3) When the temperature reaches 1383 K, magnesium vapor starts to be generated. The vapor is generated from two processes: the liquid magnesium produced in stage 2) is vaporized, and vapor is produced directly by the reduction reaction. With the generation of magnesium vapor, the reduction reaction will speed up, and the heat absorption will increase rapidly. The reaction heat also contains the latent heat of Mg vaporization. In this stage, the two related chemical equations are given as follows,

$$\mathrm{Mg}_{(l)} \longrightarrow \mathrm{Mg}_{(g)} \tag{11}$$

$$\begin{aligned} &2(\mathrm{MgO \cdot CaO})_{(s)} + (\mathrm{Fe \cdot Si})_{(s)} \\ &\longrightarrow 2\mathrm{Mg}_{(g)} + (2\mathrm{Ca \cdot SiO_3})_{(s)} + \mathrm{Fe}_{(s)} \end{aligned} \tag{12}$$

Consequently, the temperature in the retort will either increase or remain unchanged, depending on the rates of heat transfer and chemical reaction.

According to the above three stages, the reaction heat is calculated in a piecewise manner, and can be expressed as

$$S_r = \begin{cases} 0 & T < 1223K \\ -M\psi_1 \dfrac{d\alpha_1}{dt} & 1223K \le T < 1383K \\ -M(\psi_1 + \psi_2)\dfrac{d\alpha_2}{dt} - M\dfrac{\alpha_1 \psi_2}{\Delta t} & T \ge 1383K, 0 \le t < \Delta t \\ -M(\psi_1 + \psi_2)\dfrac{d\alpha_2}{dt} & T \ge 1383K, t \ge \Delta t \end{cases} \tag{13}$$

where Δt is the reaction time required for conversing the liquid magnesium into vapour in stage 3).

Control equation

Before establishing the transportation equation governing the Mg reduction, some assumptions are made,

1) Reactant compound filled into the retort is considered as solid, and the effective values of the thermophysical properties are adopted.

2) There is a large aspect ratio of height to diameter for the retort, so heat conduction in axial direction and heat radiation at the end of the retort are neglected.

Based on the above two assumptions, the magnesium reduction process in the retort is simplified as a two-dimensional, unsteady process with inner heat source, and the control equation can be expressed as

$$\frac{\partial}{\partial t}(\rho c_p T) = \nabla \cdot \lambda \nabla T + S_r \tag{14}$$

and the effective thermophysical properties of compound are listed in Table 1.

Properties	Value
Density ($\mathrm{kg \cdot m^{-3}}$)	1050~1500
Specific heat capacity ($\mathrm{J \cdot kg^{-1} K^{-1}}$)	1000~1200
Thermal conductivity ($\mathrm{W \cdot m^{-1} K^{-1}}$)	1.3
Emissivity	0.8

Table 1: Thermophysical properties of the reactant

Boundary conditions and solution method

Although the governing equation is given in the Cartesian coordinate system, for convenience, the boundary conditions is given in the polar coordinate system, and is expressed as,

$$\begin{cases} T = T_0 & r = r_0 \\ \dfrac{\partial T}{\partial r} = 0 & r = 0 \\ \dfrac{\partial T}{\partial \theta} = 0 & \theta = 0, \dfrac{\pi}{2} \end{cases} \tag{15}$$

In the above expression, T_0 is respectively 1423, 1448, 1473, and 1498 K for investigating the effect of the heating temperature on the performance of Mg reduction process.

Considering the axisymmetry of the geometry, a quarter of the whole geometry was considered as the computational domain, illustrated in Figure 1. The computational domain was discretized by structured grids, and the initial temperature is set to 300 K.

RESULTS AND DISCUSSION

Comparison with the experimental data

The above numerical model was applied to the industrial horizontal retort shown in Figure 1, which was a 300mm diameter solid cylinder. The model results in terms of Mg reduction rate are illustrated in Figure 4 and is compared with the measurements (7-12 h) (Xu and Liu,2006). The numerical results are about 8%-10% higher than the experimental data. The larger the reduction rate is, the larger is the deviation. Considering the model limitation for higher Mg reduction rate and the experimental uncertainties, the numerical results are acceptable and our model is reasonable and feasible.

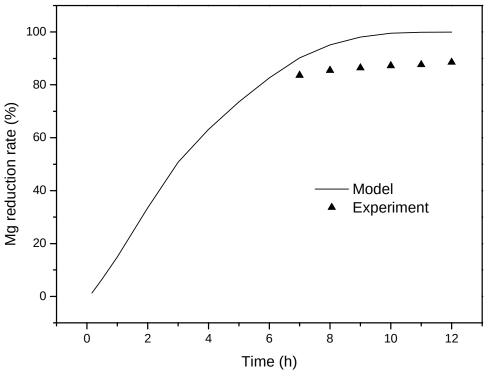

Figure 4: Comparison of model results with the measurements

Temperature distribution

For a qualitative and quantitative understanding of the heat transfer in the retort, some simulated temperature distributions of the retort are shown in Figure 5(a)-(c).

We can see that, there is a large temperature gradient at the beginning. This gradient decreases with the time due to the continuous heat conduction from the outer wall of the retort (the heat source). Figure 5(b) shows the changes of temperature distribution along the radial direction of the retort with the time. The steep curves flatten with the time, indicating temperature distribution in the retort trends to be uniform. Additionally, differentiating from the temperature increment for the same time interval in Figure 5(b), it can be concluded that there is a quick increase of temperature at first and slow increase about 2 hours later. To explain this phenomenon, a comparison of the temperature distribution for the Mg reduction process with that for a pure heat conduction process during the first 3 hours is shown in Figure 5(c). The names of curves are taken as *time* and *time-ns* (ns means no reaction) for short. *Time* represents the reaction/heating time and *ns* no reaction. During the first 30 minutes, the two curves at the

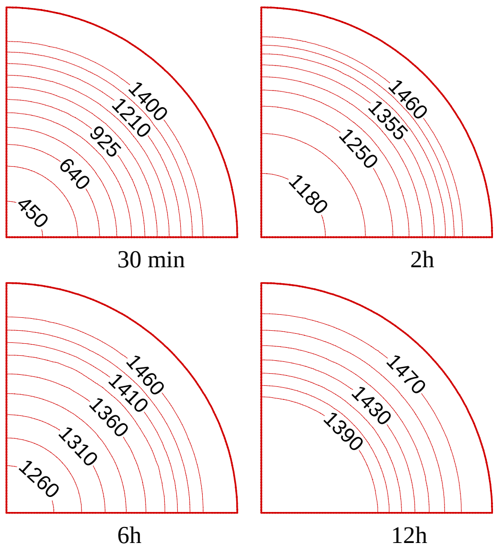

(a) Temperature profiles with the time

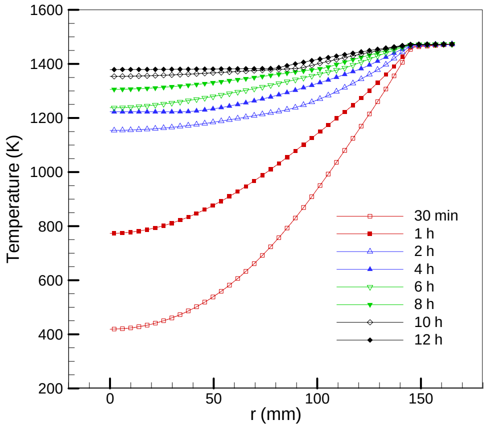

(b) Change in temperature along the radial direction of the retort with the time

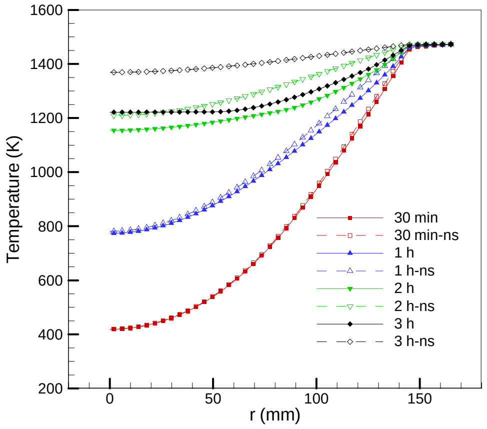

(c) Comparison of temperature for the reduction process with that for a pure heat conduction process

Figure 5: Temperature distribution in the retort

same time are almost coincident, indicating that the pure heat conduction is the dominant process, which results in a quick increase in temperature. However, 30 minutes later, there is an increasing larger deviation between the two curves at the same time, and the temperature distribution for the pure heat conduction is higher than that for Mg reduction. For the latter, the heat provided is required for Mg reduction reaction, resulting in a slow increase in temperature. It can also be inferred that the key point to improve the Mg reduction efficiency is to improve the heat conduction at this stage.

Performance of magnesium reduction process

Usually, the heating temperature on the wall of the retort placed in the furnace is not so steady and falls into a certain range. Therefore, the performance at various heating temperatures is evaluated. Figure 6 shows that the influence of the heating temperature on the performance of Mg reduction process, including the Mg reduction rate and heat absorption power. Here, the heat absorption power is defined as the ratio of the total reaction absorption power to the volume of the computational domain.

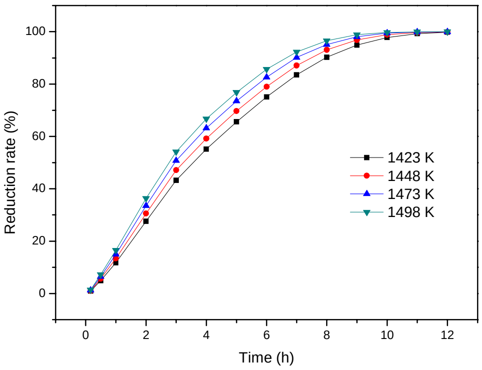

(a) Reduction rate versus time

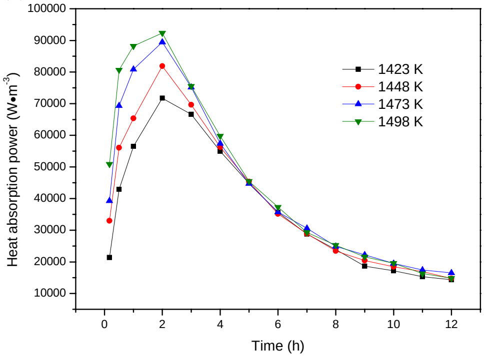

(b) Heat absorption power versus time

Figure 6: Influence of heating temperature on the performance of magnesium reduction process

From Figure 6(a), we can see that there is a lower Mg reduction rate caused by low temperature in most regions of the retort at the beginning of heating. With increasing time, more and more reactant compounds begin to react, and the corresponding reduction rate increases quickly. After a certain period, the reduction rate increases slowly because of the decreasing heat transfer rate and the consumption of the reactant. The reduction rate approximates to 100% after about 10 hours. Comparison of the curves for different heating wall temperatures shows that although they all show the similar trend, the Mg reduction rate increases when the heating temperature increases at a given time. Different from the reduction rate, the heat absorption power increases sharply at the beginning, and reaches a maximum at about 2~3 hours, and then decreases rapidly. Firstly, there is a high temperature close to the outer cylindrical wall, and the compound at this region starts to react by receiving the heat. The reaction region gradually expands with increasing temperature, resulting in a rapid increase of the heat absorption power and a maximum at about 2 hours. After this, the reduction rate becomes the dominant factor to the heat transfer, and the heat absorption power decreases gradually but has a high value. As the reactant compound is consumed gradually, the heat absorption power decreases gradually. Especially, the peaks of the heat absorption power for different heating wall temperatures occur at almost the same time but increases with increasing wall temperatures. It is obvious that the heating temperature has a large influence on the performance of Mg reduction process.

CONCLUSION

A new model for the magnesium reduction process has been developed by kinetically modifying the shrinking non-reacted core model. The calculated activation energy was fitted to the experimental data and reaction heat in a piecewise manner and found to better characterize the magnesium reduction process. The new model is applied to an industrial horizontal solid cylindrical retort, and the prediction is in general agreement with measurements.

The simulation results predict the temperature distribution in the retort and the performance of Mg reduction process in terms of Mg reduction rate and heat absorption power. During the first half hour, pure heat conduction is dominant, and the temperature of the reactant compound increases quickly resulting in a uniform temperature distribution. Both the Mg reduction rate increases and the heat absorption power increase in this period. 30 minutes later, the Mg reduction reaction becomes dominant, and the temperature increases slowly. However, the Mg reduction rate increases quickly, and the heat absorption power reaches maximum at about 2~3 hours and then decreases gradually. It is also predicted that the heating temperature has a large influence on the performance of Mg reduction process.

ACKNOWLEDGMENT

We gratefully acknowledge the financial support from the NSFC Fund (No. 50536020, 50821604).

REFERENCES

BROWN, R.E., (2009), "Magnesium in the 21st century", *Adv. Mater. Processes*, **167**, 31-3.

RAMAKRISHNAN, S. and KOLTUN, P., (2004), "Global warming impact of the magnesium produced in China using the Pidgeon process", *Resources Conservation and Recycling*, **42**, 49-64.

LIU, H.Z. and XU, R., Y. (1995), Study on the heat transfer ruler of briquette for magnesium production by the silicothermic method. Light Metals. *Light Metals*, 40-43.

MORSI, I.M., EL BARAWY, K.A., et al., (2002), "Silicothermic reduction of dolomite ore under inertatmosphere", *Canadian Metallurgical Quarterly*, **41**, 15-28.

LIANG, L., QIANG, J.F., et al. (2006). Study on deoxidizing pot interior temperature field by the silicothermic method refining magnesium technique. *Light Metals***,** 58-61.

XIE, D.H., ZHANG, G., et al. (2006), Flow effect on thermal process of magnesium reduction furnace. *Journal of University of Science and Technology Beijing***,** 566-569.

YU, A., HU, H., et al., (2002), "Mathematical modelling of magnesium reduction in a novel vertical Pidgeon process", *Modelling and Simulation in Materials Science and Engineering*, **10**, PII S0965-0393(02)36337-X.

XIONG, C.H., ZHOU, T.R., et al. (2005). Factors affecting the reduction process in smelting magnesium with Pidgeon process. *Southern Metals***,** 1-4.

XU, R.Y. and YUAN, H.B. (1991), A mathematical analysis of the influence of factors on the magnesium reduction rate and silicon utilization rate for magnesium production by the silicothermic method. *Light Metals***,** 43-46.

HALMANN, M., FREI, A., et al., (2008), "Magnesium production by the pidgeon process involving dolomite calcination and MgO silicothermic reduction: Thermodynamic and environmental analyses", *Industrial & Engineering Chemistry Research*, **47**, 2146-2154.

XU, R.Y. and LIU, H.Z. (2006), The gradient of reaction conditions for making magnesium with siliconthermic process. *Light Metals***,** 44-47.